Robotica (2016) volume 34, pp. 995–1009. © Cambridge University Press 2014
doi:10.1017/S026357471400201X

USV attitude estimation: an approach using quaternion in direction cosine matrix

Chiemela Onunka*, Glen Bright and Riaan Stopforth

Discipline of Mechanical Engineering, University of KwaZulu-Natal, KwaZulu-Natal, South Africa

(Accepted June 26, 2014. First published online: July 31, 2014)

SUMMARY

Positioning and navigation data for unmanned surface vehicles (USVs) are extracted using the Global Positioning System (GPS) and the Inertial Navigation System (INS) integrated with an inertial measurement unit (IMU). The integration of quaternion with direction cosine matrix (DCM) with the aim of obtaining high accuracy with complete system independence has been effectively used to supply position and attitude information for autonomous navigation of marine crafts. A DCM integrated with a quaternion provided an advanced technique for precise USV attitude estimation and position determination using low-cost sensors. This paper presents the implementation of an INS developed by the integration of DCM and quaternion.

KEYWORDS: Inertial measurement unit; Inertial navigation system; Quaternion, Direction cosine matrix.

1. Introduction

It has become a standard procedure to equip unmanned surface vehicles (USVs) with Global Positioning System (GPS) to provide accurate position and velocity data for autonomous navigation.[1] The convergence of position data management systems and communication technologies has induced the need for improvement in the development of reliable in-vehicle navigation and guidance systems.[1] There has been an increase in the use of automation in boats, ships and other marine vehicles for scientific, military and commercial purposes. This has led to an improvement in the operational reliability, efficiency and safety of marine vehicles.[2–3] The interest in the use of USVs for the purpose of search and rescue has been growing with particular emphasis on reliable, accurate and continuous availability of attitude data for attitude control.[4] Enhancing the safety and performance of marine vehicles is important in the development of marine craft. This has influenced the development of intelligent systems. These systems are used by marine vehicles to gather actual information from the environment. The data gathered are used to predict the marine craft motion while ensuring optimal performance of the craft.[5]

Different categories of marine vehicles require continuous and precise navigation. They also require position information, with the integrity of the navigation and positioning system being key factors in the performance of marine vehicle.[6] Different navigation algorithms have been developed over the years to provide navigation and position data for unmanned systems. These have been used in the control of autonomous vehicles.[7] Interests in developing and using integrated navigational systems have initiated several navigation support systems that are widely in use today.[2,5]

Research in navigation algorithms and advancements in control engineering offer techniques in determining large-scale changes, which may occur in the positioning and navigation of marine vehicles.[3] The angular rates and accelerations computed using Inertial Measurement Unit (IMU) are integrated by the Inertial Navigation System (INS) algorithm to obtain the position, velocity and attitude of marine vehicle. As a result of IMU inaccuracies and integration errors, the solutions obtained diverge quickly.[15] This prompts the need for closed-loop systems to stabilize the integration. Integration of INS is usually done with a Complementary Kalman Filter (CKF) or an Extended Kalman

* Corresponding author. Email: connadoz@gmail.com

Filter (EKF).[8] Integrating quaternion with direction cosine matrix (DCM) provides a technique for obtaining high accuracy in short time intervals with complete system independence. This has been used to supply position and attitude information for autonomous navigation of marine crafts.[20]

This paper presents the implementation of DCM and quaternion in providing an advanced technique for precise USV position, attitude estimation and determination. This was done using low-cost sensors. The navigation system algorithm was based on the integration of precise INS with GPS using data from gyros. Drifts in the INS were compensated for by using GPS, digital compass and accelerometers. The rationale in using DCM in attitude estimation and determination was to attain the next level in stabilization and control of USV. Thus, an essentially stable marine craft with rudder control was converted to a USV, controlled using a range of stabilizing sensors.[9] A DCM was derived from the information streaming in from the gyros. This information formed the rotation matrix of marine vehicle. The coordinate system of marine vehicle was located at the centre of gravity of the craft. A vector in the body coordinate system of the craft was transformed into another coordinated system through the multiplication of the vector by the rotation matrix. The reverse transformation of the vector was achieved through the multiplication of the new vector by the inverse of the rotation matrix. The quaternion was computed from initial inputs and values arising from the rotation matrix.[9] It should be noted that it is outside the scope of this paper to delve into comparison between Kalman filter and DCM.

2. Literature Review

Advancements in navigation algorithms use low-cost IMUs to provide position, velocity and vehicle attitude solutions that are reliable.[16,22] Such navigational algorithms make use of different complementary filters to ensure global stability of the navigation algorithm. A complementary filter was used in the DCM computational algorithm to provide stability in the navigation algorithm. Complementary filters provide ways of fusing noisy signals that have complementary spectral properties.[23] A direct complementary filter uses a nonlinear observer obtained from quaternion formulation. A passive complementary filter uses nonlinear equations to predict angular velocity components in an estimator frame of ref. [24]. The representation of passive complementary filter using direct data obtained from an IMU describes an explicit complementary filter. Explicit complementary filters are used for attitude estimation on low-pass filtering to obtain low-frequency attitude estimates. The low-pass filter inputs are obtained from accelerometer and the gyro data.[10]

These filters can be used in special orthogonal groups in attitude estimation and computation.[11] The different implementations of the filters can bring about exponential convergence of the navigation algorithm.[12] The performance of filters has proved to be advantageous in DCM algorithm formulation. There has been an increased use of coupled nonlinear attitude estimation and control for attitude stabilization using low-cost IMU on USVs.[13] To maximize the potential of low-cost IMU, it was necessary to perform multisensory data fusion DCM computational processes with an IMU and a GPS. Integrating low-cost IMU into the navigation algorithm for marine vehicle and using DCM as a computational engine for attitude estimation allowed for fast calibration and alignment of the INS. The INS was optimized for marine vehicle navigation. The end results from DCM were also achieved by using the Kalman filtering process.[4,6,14] The filtering algorithm can be adaptive to the system. This makes it possible for errors arising from the algorithm to be reduced.[2]

3. Numerical Analysis

Marine vehicle motion on open waters was described by its translational and rotational motion characteristics. The movement of the centre of gravity of marine vehicle was used to describe the translational motion. Movements around the centre of gravity of marine vehicle were used to represent the rotational motion.[20] A fixed axis placed on the body of marine vehicle enabled an adequate representation of the orientation of the vehicle with respect to the earth-fixed frame of reference. The orientation of marine vehicle was indicated through rotations about the fixed axis.[19] Orientations of marine craft were generally kept in check through the use of nonlinear differential equation. The nonlinear differential equation described marine vehicle's kinematics.[9] The marine vehicle kinematics represented an application of Newton's laws to the time rate of change of vector

https://doi.org/10.1017/S026357471400201X Published online by Cambridge University Press

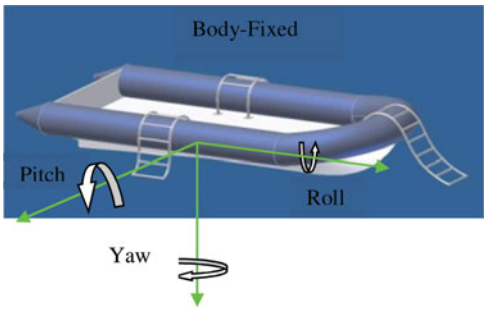

Fig. 1. USV coordinate system.

rotation with respect to applied torques and moments. This provided insights into the rotation of marine vehicle as a rigid body. It also expressed different ways in which the rotations transformed from one coordinate system to another.

The USV maintained the relevant properties of the coordinate system during coordinate system transformation. Nonlinear differential equations were used to represent the marine vehicle kinematics. It also expressed the rigid body rotations about the fixed body axis. The time evolution of the orientation of marine vehicle with respect to its vector rotation rate was represented by the marine vehicle kinematics.[9] Integrating the nonlinear differential equation enabled the use of a series of matrix compositions. Numerical errors were introduced with the use of numerical integration in the computational analysis of the marine vehicle kinematics. This does not yield the same result as symbolic integration. The representation of exact gyro data with precise symbolic integration produced an accurate rotation matrix. Errors were generated from the use of exact gyro data without using precise symbolic integration.[18]

Integration error: The use and implementation of finite step time in sampling IMU data at a finite sampling rate involved a numerical integration process. This generated numerical errors in the computation and analysis of IMU data.[25] Different methods were used to analyse the process. This allowed for certain assumptions to be made about the data samples during integration. A constant rotation rate of marine vehicle over step-time provided a useful assumption and technique in the analysis of integration error. The error introduced in the computation and analysis of the integration error was proportional to the rotational acceleration of the vehicle.[26]

Quantization error: Digital representations of IMU data values were finite. This introduced quantization errors in the navigation algorithm.[27] Quantization errors start at the analog to digital converter in the microcontroller and build up during the computation of data. These do not preserve all the navigational data.[28]

4. Axis Representation

Attitude estimation and determination for marine vehicle was focused on the body-fixed frame of reference (b-frame). This allowed for approximations and assumptions on the location of the centre of gravity of marine vehicle. Euler angles were used to represent the angular rotation of marine vehicle about the b-frame of reference. The frame of reference is shown in Fig. 1. The following rotations were possible in the body-fixed coordinate system describing Euler angles in the frame of reference:

1. Rotations about the x-axis expresses the roll angle φ.
2. Rotations about the y-axis expresses the pitch angle θ.
3. Rotations about the z-axis expresses the yaw angle ψ.

These are represented in the vector form as follows:

$$\Phi_{nb} \underline{\underline{\Delta}} \begin{bmatrix} \varphi \\ \theta \\ \psi \end{bmatrix}, \tag{1}$$

https://doi.org/10.1017/S026357471400201X Published online by Cambridge University Press

and the rotation matrix is expressed as

$$R\left(\Phi_{nb}\right) = \begin{bmatrix} c\psi c\theta & -s\psi c\varphi + c\psi s\theta s\varphi & s\psi s\varphi + c\psi c\varphi s\theta \\ s\psi\, c\theta & c\psi c\varphi + s\varphi s\theta s\psi & -c\psi s\varphi + s\psi c\varphi s\theta \\ -s\theta & c\theta s\varphi & c\theta c\varphi \end{bmatrix}. \tag{2}$$

Considering the linear transformation of marine vehicle which expressed vehicle dynamics in 3-degree-of-freedom, the position and heading of marine vehicle is expressed as:

$$\eta = [x, y, \psi]^T. \tag{3}$$

The velocity vector is expressed as:

$$\nu = [u, v, r]^T. \tag{4}$$

The rotation matrix expressed as a function of the marine vehicle heading is

$$R\left(\psi\right) = \begin{bmatrix} \cos(\psi) & -\sin(\psi) & 0 \\ \sin(\psi) & \cos(\psi) & 0 \\ 0 & 0 & 1 \end{bmatrix}. \tag{5}$$

The rotation of the velocity vector in the earth-fixed coordinate system is represented as:

$$\dot{\eta} = R(\psi)\nu. \tag{6}$$

5. DCM Formulation

Nonlinear differential equations of motion provided the platform in which DCM was computed. The time rate of change of direction cosines has a distinct relationship with the gyro signals. The aim in using inputs from gyro to compute direction cosines was to make appropriate approximations. The approximations maintained and kept in check the nonlinearity of the equations of motion. A mechanical gyro has the disadvantage of being fixed in a particular position and space. Electronic gyros provided the required outputs as they rotated with marine vehicle. Outputs from the electronic gyros were proportional to the turning rates of marine vehicle. A direct integration and implementation of gyro signals did not produce the required results as gyro rotations are not commutative. This is due to the importance of the sequence of rotation in the computation of DCM.[18] The kinematics of rotations indicates that the rate of change of a rotating vector due to its rotation is denoted as:

$$\frac{dr(t)}{dt} = \omega(t) \times r(t), \tag{7}$$

where $\omega(t)$ represents the rotation rate of the vector. This is equivalent to the rotation rate of the rotation matrix. The following observations were made in the use of Eq. (7).

1. Equation (7) is a nonlinear differential equation whose nonlinearity was maintained in the DCM computation. Rotation vector inputs were cross-multiplied with a variable that was integrated at a later stage in the computation of DCM. Linear methods were used in Eq. (7) by applying appropriate approximations.
2. The vectors in Eq. (7) were measured in the same coordinate system or frame of reference.
3. The order of the resulting components of the matrix was reversed and the signs changed. This was because the cross products of the vectors in Eq. (7) were anti-commutative.

Information from the initial conditions and time history of the rotation vector facilitated the numerical integration of the cross product of rotating vectors. This was used to track the rotating

https://doi.org/10.1017/S026357471400201X Published online by Cambridge University Press

vector in the following process:

$$r(t) = r(0) + \int_0^t d\theta(\tau) \times r(t), \tag{8}$$

where

$$d\theta(\tau) = \omega(\tau) d\tau, \tag{9}$$

$r(0)$ indicates the starting value of the vector, $\int_0^t d\theta(\tau) \times r(t)$ is the change in the vector.

The elements of the rows and columns of the rotation matrix were regarded as rotating vectors. This assumption created a model that resolved the differences in rotations that occur in a body-fixed coordinate system and an earth-fixed coordinate system. The symmetry property in the rotation matrix was used while considering the above assumption. The earth-fixed coordinate system rotated in equal and opposite directions to the rotation of the body-fixed coordinate system in the earth-frame of reference. The earth-frame of reference was tracked from gyro signals by simply changing the signs of gyro signals. The rotation matrix elements resulting from the cross-product computations were interchanged and the signs changed back again,[9]

$$r_{\text{earth}}(t) = r_{\text{earth}}(0) + \int_0^t r_{\text{earth}}(\tau) \times d\theta(\tau), \tag{10}$$

where $d\theta(\tau) = \omega(\tau) d\tau$ and $r_{\text{earth}}(t)$ indicates the earth axis as seen by marine vehicle. By using and implementing the same matrix manipulation used by Euston and Mahony,[10,11,13] Eq. (10) was represented as:

$$r_{\text{earth}}(t + dt) = r_{\text{earth}}(t) + \int_0^t r_{\text{earth}}(t) \times d\theta(t), \tag{11}$$

where $d\theta(t)$ represents $\omega(t)dt$. The correction made to the rotation rate of gyro measurements was taken from the proportional and the integral elements of the drift compensation feedback controller. This was done to produce an adequate estimate of the true rotation rate of marine vehicle,

$$\omega(t) = \omega_{\text{gyro}}(t) + \omega_{\text{correction}}(t). \tag{12}$$

$\omega_{\text{gyro}}(t)$ in Eq. (14) is the three-axis gyro measurements and $\omega_{\text{correction}}(t)$ is the gyro correction component fed back to the controller. In the computation of DCM components, accelerometers and GPS were used as reference vectors. They were used to compute rotational error. The result from the rotational error computation was then fed back into the computation. This was also fed into the rotation matrix update sequence through a feed back controller. Equation (10) was used in the feed back control process. The computation of Eq. (10) was repeated for each of the earth fixed axes and the result is presented as:

$$R(t + dt) = R(t) \begin{bmatrix} 1 & -d\theta_z & d\theta_y \\ d\theta_z & 1 & -d\theta_x \\ -d\theta_y & d\theta_x & 1 \end{bmatrix}, \tag{13}$$

where $d\theta_x = \omega_x dt$, $d\theta_y = \omega_y dt$, $d\theta_x = \omega_x dt$. Equation (13) was used in updating the DCM components using inputs from gyro signals. The above result can be compared with the result obtained by Euston and Mahony.[10,11,13] The terms having the value of one in the diagonal of the matrix in Eq. (13) indicate the first term in Eq. (11). The second term in Eq. (11) indicates smaller off-diagonal components of the matrix. The implementation of Eq. (13) was done through repeated matrix multiplications with short time steps. Twenty-seven matrix multiplications and 18 additions were required for each matrix multiplication.[10,11,12,18] To maintain the integrity of the matrix in each time step, approximations were made to shorten the time steps to about 0.015 s. A maximum change in the components of the rotation matrix were made within 1.5 to 2% of the time step such that the second-order terms that arose were ignored within the same time range. The use of Eq. (13) by itself

https://doi.org/10.1017/S026357471400201X Published online by Cambridge University Press

without gyro signals accumulated gain errors, gyro drift offset and numerical round-offs. Using Eq. (11), the gyro signals yielded the desired result with very low gyro drift and improved performance.

5.1. Renormalization of matrix

Numerical errors reduce the orthogonal properties of the rotation matrix to approximations rather than identities.[29] The effect of this reduction is that the earth coordinate system and the body-fixed coordinate system are no longer describing the motion of marine craft in space. Numerical errors accumulate at a very slow rate and this creates the conditions that enforce and reinforce the conditions of matrix orthogonality.[10] This process is the renormalization of the rotation matrix. This is done by computing the dot product of X and Y rows of the rotation matrix. The computation effectively measures by how much X and Y rows are rotating towards each other,[11]

$$X = \begin{bmatrix} r_{xx} \\ r_{xy} \\ r_{xz} \end{bmatrix} \quad Y = \begin{bmatrix} r_{yx} \\ r_{yy} \\ r_{yz} \end{bmatrix}, \tag{14}$$

$$\text{error} = X \bullet Y = X^T Y = \begin{bmatrix} r_{xx} & r_{xy} & r_{xz} \end{bmatrix} \begin{bmatrix} r_{yx} \\ r_{yy} \\ r_{yz} \end{bmatrix}. \tag{15}$$

Each of the X and Y rows are allocated half of the errors, and they are also rotated in the opposite direction by cross coupling,

$$\begin{bmatrix} r_{xx} \\ r_{xy} \\ r_{xz} \end{bmatrix}_{\text{orthogonal}} = X_{\text{orthogonal}} = X - \frac{\text{error}}{2} Y, \tag{16}$$

$$\begin{bmatrix} r_{yx} \\ r_{yy} \\ r_{yz} \end{bmatrix}_{\text{orthogonal}} = Y_{\text{orthogonal}} = Y - \frac{\text{error}}{2} X. \tag{17}$$

Allocating equal gain values to each of the X- and Y-row vectors resulted in lower residual error after correcting and updating the matrix. This was not the case if the error was allocated only to the row vectors of the matrix. The next stage of computations involved the adjustment of the Z row of the rotation matrix to comply with the orthogonality requirement of the matrix. The Z row was adjusted such that it was orthogonal to both X and Y rows. This was done by equating the Z row to the cross product of X- and Y-row vectors,

$$\begin{bmatrix} r_{zx} \\ r_{zy} \\ r_{zz} \end{bmatrix}_{\text{orthogonal}} = Z_{\text{orthogonal}} = X_{\text{orthogonal}} \times Y_{\text{orthogonal}}. \tag{18}$$

The last step in the rotation matrix renormalization process involved scaling the row vectors in the rotation matrix. This was done to achieve a magnitude of unity in each of the components of the matrix. To scale the matrix elements, each of the row components were divided by the square root of the sum of the squares of the elements in that row. Taylor's expansion was applied to the scaling, bearing in mind that the magnitudes of the matrix components may not be greater than one. This resulted in magnitude adjustment equations for row vectors,

$$X_{\text{normalized}} = \frac{1}{2} \left(3 - X_{\text{orthogonal}} \bullet X_{\text{orthogonal}}\right) X_{\text{orthogonal}}, \tag{19}$$

$$Y_{\text{normalized}} = \frac{1}{2} \left(3 - Y_{\text{orthogonal}} \bullet Y_{\text{orthogonal}}\right) Y_{\text{orthogonal}}, \tag{20}$$

https://doi.org/10.1017/S026357471400201X Published online by Cambridge University Press

$$Z_{\text{normalized}} = \frac{1}{2}\left(3 - Z_{\text{orthogonal}} \bullet Z_{\text{orthogonal}}\right) Z_{\text{orthogonal}}. \tag{21}$$

The result generated by the above equations implied that the magnitude of each row vector was adjusted to unity. The row vector adjustment was done by subtracting the dot product of the vector from itself, subtracted from three, multiplied by a half and then multiplying each element by the result. The computations for each step of the integration are within 0.020 s.[18]

5.2. The quaternion

Due to the usage of Euler angles in rotation matrix computations, singularities occur in the rotation matrix computations. Singularities can be avoided if the rotation matrix is treated as having orthonormal row vectors as discussed in earlier sections. Singularities can also be avoided by using quaternion to compute the elements of the rotation matrix. Quaternion arose from the transformation between Euler angles and Euler parameters. The transformation resolves the problem of singularity that existed with the use of Euler angles even though they were more intuitive and readily available to use.[13] Given that Euler angles θ, φ, ψ are known, the quaternion $q = [\varepsilon_1, \varepsilon_2, \varepsilon_3, \eta]^T$ was computed through the following matrix manipulations[19]:

$$R_1 = \begin{bmatrix} R_{11} & R_{12} & R_{13} \\ R_{21} & R_{22} & R_{23} \\ R_{31} & R_{32} & R_{33} \end{bmatrix}, \tag{22}$$

$$R_{44} = \sum_{i=j}^{3} R_{jj}, \tag{23}$$

$$|P_4| = \sqrt{1 + 2R_{44} - R_{44}}, \tag{24}$$

$$P_1 = \frac{R_{32} - R_{23}}{P_4} \quad P_2 = \frac{R_{13} - R_{31}}{P_4} \quad P_3 = \frac{R_{21} - R_{12}}{P_4}, \tag{25}$$

$$e = [e_1, e_2, e_3, e_4]^T = [\varepsilon_1, \varepsilon_2, \varepsilon_3, \eta]^T. \tag{26}$$

Hence,

$$e_1 = \varepsilon_1 = \frac{P_1}{2} \quad e_2 = \varepsilon_2 = \frac{P_2}{2}, \quad e_3 = \varepsilon_3 = \frac{P_3}{2} \quad e_4 = \eta = \frac{P_4}{2}, \tag{27}$$

and the new rotation matrix free of singularities is presented as:

$$E(e) = \begin{bmatrix} 1 - 2\left(\varepsilon_2^2 + \varepsilon_3^2\right) & 2\left(\varepsilon_1\varepsilon_2 - \varepsilon_3\eta\right) & 2\left(\varepsilon_1\varepsilon_3 + \varepsilon_2\eta\right) \\ 2\left(\varepsilon_1\varepsilon_2 + \varepsilon_3\eta\right) & 1 - 2\left(\varepsilon_1^2 + \varepsilon_3^2\right) & 2\left(\varepsilon_2\varepsilon_3 + \varepsilon_1\eta\right) \\ 2\left(\varepsilon_1\varepsilon_3 + \varepsilon_2\eta\right) & 2\left(\varepsilon_2\varepsilon_3 + \varepsilon_1\eta\right) & 1 - 2\left(\varepsilon_1^2 + \varepsilon_2^2\right) \end{bmatrix}. \tag{28}$$

Equation (28), which represents the new rotation matrix, was used as the basis of DCM computation.

5.3. Euler parameters and singularities

Euler angles and Euler parameters were used to describe the orientation of marine vehicle as they were more intuitive and are frequently used parameters in the description of rigid body orientation. It was convenient to use the Euler angle representation. The three Euler parameters correspond to roll, pitch and yaw angles of marine vehicle. These parameters were not global in their usage without matrix singularities. As a result of singularities being present and also a property of Euler angles, pitch angles, $\theta = \pm 90^\circ$, were not defined. For practical purposes, these angles cannot be reached as a result of the meta-centric restoring forces of marine vehicle. The "wraparound" effect associated with the Euler angle representation implied that Euler angles can be integrated up to the values outside the $\pm$ 90° range of pitch and $\theta = \pm$ 180° range of roll and yaw. This problem was addressed with the described matrix renormalization procedure that was adopted.

https://doi.org/10.1017/S026357471400201X Published online by Cambridge University Press

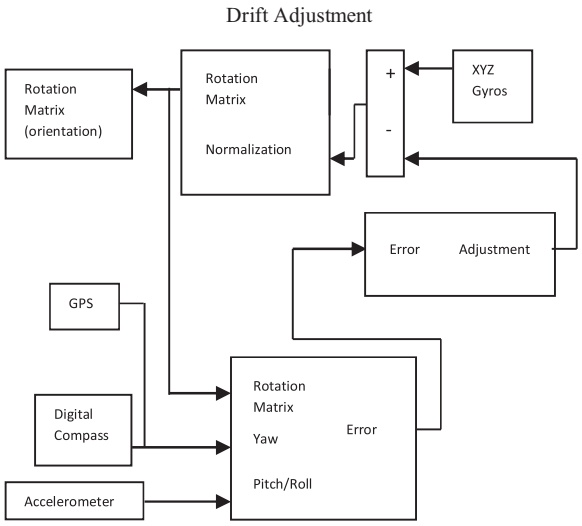

Fig. 2. DCM block diagram.[18]

To avoid singularities and "wraparound" problems, a parameter description known as quaternion based on Euler parameters was applied to the rotation matrix. The advantage of using quaternion was in the representation and computational efficiency of the rotation matrix. The computations involved sets of numerical integrations using sets of nonlinear differential equations.[19]

5.4. Drift correction

Gyro signal drift correction, as shown in Fig. 2, used the orientation of the reference vector with no drift characteristics. The feedback loop shown in Fig. 2 indicated the model and pattern in which the microcontroller was programmed to achieve real time results. The reference vectors were provided with accelerometers and the GPS system. The transient properties of gyro signals were the point of focus in drift correction process. Hence, little or no attention is paid to the transient properties of the reference vector. The performances of gyros were manageable with an uncorrected offset in the order of few degrees per second. The detection of gyro offsets involved the comparison of orientation references with gyro signals. This provided a negative feedback loop to gyro to account and compensate for errors in gyro signals as shown in Fig. 2. The procedure used in the gyro drift correction is as follows:

1. Data are first received from gyro.
2. Rotation vectors were aligned, measured and computed. Values of reference vectors were computed. This enabled the use of orientation reference vectors to detect orientation error.
3. The detected orientation error vectors were fed back into the loop through a PI feedback controller to produce the required rotation rate adjustment for gyros.
4. Depending on the sign convention of the rotation error, the output from PI controller was added or subtracted to real gyro signals.
5. The procedure was repeated again in a loop.

Global Positioning System and accelerometers were important devices used as reference vectors. Accelerometer provided the reference vector for the roll and pitch axis of marine vehicle. The yaw axis reference vector was provided by GPS. The cross products of estimated and measured vectors from DCM were used for the computation and detection of orientation error. Cross products of vectors were computed. The magnitude of the cross products was proportional to the sine of the angle between the vectors and the direction of the product perpendicular to the vectors. The result indicated the amount of rotation required by the measured vector to be parallel to the estimated vector. The result was fed back for comparison with gyro signals through PI controller. This indicated an equivalent negative orientation error. It forced the estimated orientation to track reference vectors.

Drifts in gyro signals were corrected from these processes.[21] The cross product of the measured reference vector computed with an equivalent vector from DCM indicated the orientation error.

https://doi.org/10.1017/S026357471400201X Published online by Cambridge University Press

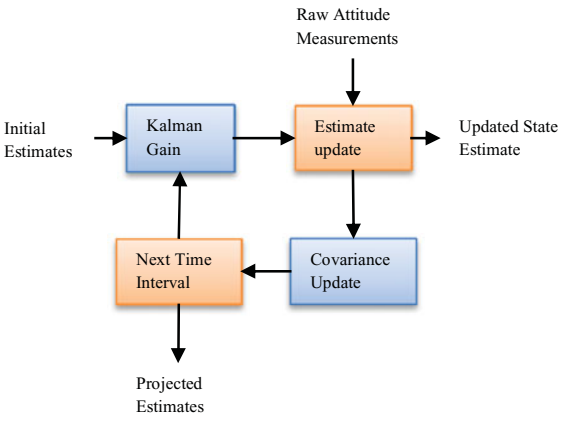

Fig. 3. Kalman filter recursive algorithm.

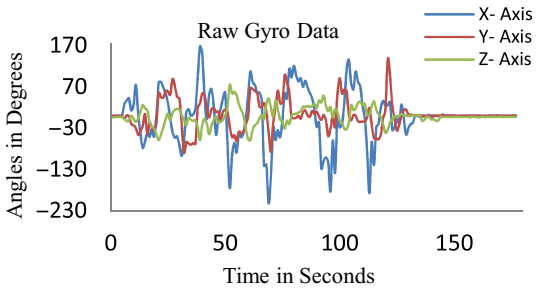

Fig. 4. Gyro readings.

An approximate equivalence to the rotation matrix was required to bring the reference vector into alignment with the computed vector.[18] The number of rotations required for vector alignment is an important factor in computations. The correctional rotation vector was computed from the cross product of estimated and reference vectors mapped in DCM. The PI feedback controller also has a functional requirement of cancelling thermal drift with zero residual orientation error and gyro offsets. The mapping of reference vectors with gyro signals through DCM was dependent on the orientation of IMU,[22]

$$\text{Total Correction} = W_{RP}\text{Roll/Pitch Correction Plane}. \tag{29}$$

This is then fed into PI controller,

$$\omega_{P\ \ \text{Correction}} = K_P\ \ \text{Total Correction}, \tag{30}$$

$$\omega_{I\ \ \text{Correction}} = \omega_{I\ \ \text{Correction}} + K_I dt\ \ \text{Total Correction}, \tag{31}$$

$$\omega_{\text{Correction}} = \omega_{P\ \text{Correction}} + \omega_{I\ \text{Correction}}. \tag{32}$$

5.5. Accelerometer

Acceleration and gravity quantity were measured with an accelerometer. This measurement device enabled the measurement of linear movements in the fixed-body reference frame of marine craft. Accelerometer was important in the correction of roll and pitch drifts because it has zero drift in its outputs. The implementation of accelerometer in navigation algorithm provided forward acceleration and deceleration of marine craft, in addition to roll-pitch drift correction. Accelerometer signals shown in Fig. 4 have the characteristic of not accumulating errors in the same manner as gyro signals in Fig. 3. There are no drifts in the output of an accelerometer. The properties of accelerometer allowed it to produce direct measurement of orientation instead of time-rate of change of orientation.

https://doi.org/10.1017/S026357471400201X Published online by Cambridge University Press

5.6. Ocean waves and wind

The effects of wind and waves on the DCM navigation algorithm played an important role in keeping the marine vehicle on course. The effects of ocean waves and wind were regarded as drifts in navigation algorithm. These forces in nature gradually cause marine vehicle to rotate and go off course. Feedback gains were used to adapt the controller to counteract the effects of winds and waves in situation where marine vehicle was off course.[9]

6. DCM Navigation and Control

The guidance, navigation and control of marine vehicle in the Cartesian frame of reference were achieved by implementing cross products and dot products of vectors generated in the frame of reference by the following procedure:

1. The data representing the pitch attitude were used to control the pitch of marine vehicle. This was computed from the dot product of the roll axis of marine vehicle with the vertical axis associated with the earth-centered frame of reference. The dot product of the roll axis with the yaw axis represented the direction matrix component, r_{zx}. This was also represented by the sine angle between the pitch axis and the earth-fixed reference plane.
2. The roll of marine vehicle was controlled from the roll attitude data. The roll attitude data were computed from the dot product of the pitch axis on marine vehicle with the earth-centered vertical axis. The direction matrix component r_{zy} represented the dot product of the pitch axis with the vertical axis. This was also represented by the sine angle between the pitch axis and the horizontal in the earth-fixed frame of reference.
3. Data from yaw attitude were used in navigating the marine vehicle in the desired course. The yaw attitude was computed from the cross product of the roll axis of marine vehicle with a vector in the desired course and heading. The dot product of the roll axis taken with the desired course yielded the opposite motion of marine vehicle in the opposite direction of the desired course. Negative values from the computation indicated 90° off course by marine vehicle.
4. The turning rate of marine vehicle about the z-axis was determined from the transformation of the gyro rotation vector to the earth-fixed reference frame. Dot product of the result was then computed with the vertical axis. The computation of marine vehicle's turning rate was represented by

$$\omega_x r_{zx} + \omega_y r_{zy} + \omega_z r_{zz}. \tag{33}$$

6.1. GPS navigation

Global Positioning System provided drift-free reference vector required for yaw orientation correction. Every second GPS provided data representing the magnitude and direction of marine vehicle. Orbiting satellites in space transmitted GPS signals containing information about the location and velocity of marine vehicle. The GPS receiver transmitted data in NMEA format, which was delimited by commas in readable ASCII format. Accurate data regarding marine craft heading were achieved as the GPS receiver was also in motion with marine vehicle. The marine vehicle velocity vector was transmitted to microcontroller from GPS at per second interval. This represented change in the position of GPS antenna per second. The GPS unit provided velocity and position of marine vehicle in two coordinates. The first coordinate has GPS signals containing the longitude, latitude, altitude, velocity and course over ground. The angle of the desired course measured in clockwise direction from North represented the course over ground. This was also equivalent to the angle computed mathematically in counter-clockwise direction around the z-axis of the marine vehicle body fixed frame of reference. The GPS sent position and velocity data with the origin of the X, Y, and Z frames of reference at the centre of the earth.

6.2. GPS signal characteristics and dynamics

The following properties were exhibited by the transmitted GPS signals:

https://doi.org/10.1017/S026357471400201X Published online by Cambridge University Press

1. *Latency*: In certain operational conditions, the GPS unit took 10 s or more before transmitting any data. This resulted in the delay in the transmission of position data.
2. *Filtering*: GPS units had an embedded filter. The filter improved the accuracy of position and velocity data estimation. This provided a smoothing effect on the transmitted data when GPS changed its position or velocity. The new data were received in 2 ms as a result of smoothing effect.
3. *Static navigation and path smoothing*: GPS had a radio embedded in its design. This radio enabled GPS to ignore abrupt changes in position and velocity data. This provided path smoothing effect for navigation setup. The option of static navigation was used in situations where perceptible variations in location were concealed, given that the velocity fell below a certain value. These two options were mostly set as default by the manufacturer.

In 1 s, an exponential response of GPS unit was produced from its dynamic response. The step change took roughly about 3 s for completion. A small error was introduced in GPS computation if the dynamic response of GPS was ignored. To compensate for this error, a filter was designed with GPS and introduced between DCM and input to yaw drift correction. The GPS navigation algorithm assumed that the marine craft moved or followed the specified heading and direction. Transient errors in the above assumption physically do not have any impact on the performance of the algorithm. Drift correction in the DCM algorithm was not only achieved through the use of GPS signal. This was also achieved by using a magnetometer or a digital compass. Strong winds and ocean waves violated this assumption. To ensure that the assumption was accurate, moderate feedback gains were applied to the control system. The error at the input of the drift correction feed back was represented by the difference between the desired heading of marine vehicle and current heading. This allowed DCM to adapt to changes caused by wind and waves. The marine vehicle was rotated by the amount required to keep it travelling along the desired course.[9]

7. DCM versus Kalman Filter

Kalman filter is a variant of an optimal mean square error algorithm.[17] It utilized state space methods in the determination and computation of estimates and predictions. State space definitions of problems allowed for the implementation of Kalman filter in discrete domain. Kalman's recursive algorithm allowed for state space estimates as shown in Fig. 3. USV attitude estimates were determined using Kalman filter. Results from Kalman filter are shown in Figs. 9 and 10. The DCM algorithm when compared with a known algorithm, such as Kalman filter, used 5% of microcontroller capacity. The floating point computations associated with the Kalman filter algorithm were usually intense for the microcontroller running at low megahertz. The DCM algorithm performed more efficiently than the simple Kalman filter algorithm. It is matched in efficiency only by the extended Kalman Filter algorithm. The results shown in Figs. 6 and 7 are appreciated more when the results were compared with the actual physical rotation of marine vehicle in real time.

Figure 8 shows the performance of a complementary filter included in the DCM algorithm. Rotation in the yaw axis from $+180^\circ$ to -180° degrees depicted the smoothing effect of the complementary filter included in the algorithm. Low-pass filtering of IMU data required the fusion of complementary filter data with low-frequency certainty of the marine vehicle attitude and raw gyro data. To provide for a more reliable data and measure of improvement, the IMU data were averaged. Ideally, the average error should be zero. A non-zero average error indicated low frequency. This reduced the performance of complementary filter.

8. Results

The research results showed and demonstrated the practical efficiency of quaternion and matrix renormalization in the DCM computation of the marine vehicle attitude for autonomous navigation. Integrating low-pass complementary filters with accelerometers provided faster response from the algorithm. This allowed gyro data to be obtained efficiently as shown in Fig. 8. The results were accessed in real time. The results shown in Figs. 4 to 8 were obtained from making rotation predominantly along the yaw axis.

https://doi.org/10.1017/S026357471400201X Published online by Cambridge University Press

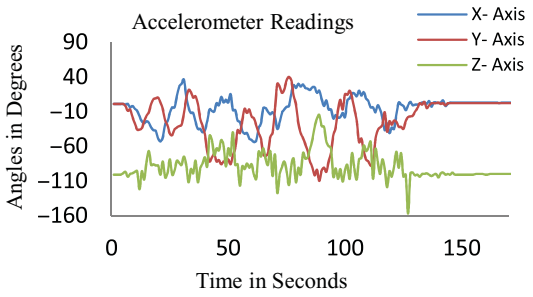

Fig. 5. Accelerometer values.

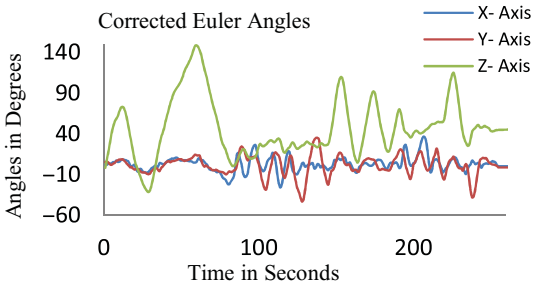

Fig. 6. Corrected marine craft attitude.

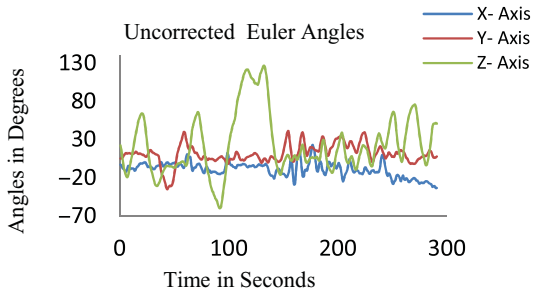

Fig. 7. Uncorrected marine craft attitude.

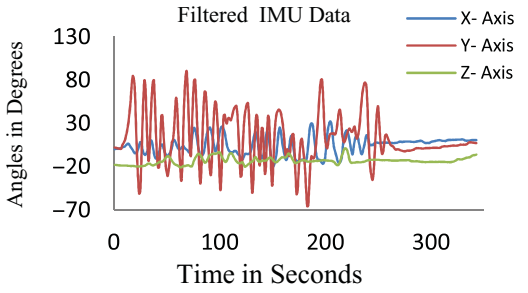

Fig. 8. Filtered IMU data.

Figures 4 and 5 showed the extent of noise present in raw signals streaming in from gyro and accelerometer. Figure 6 showed the corrected Euler angles using accelerometer for roll and pitch correction and GPS or magnetometer for yaw correction. Figure 7 showed the uncorrected Euler angles. The corrections were the result of the implementation of matrix renormalization and quaternion in matrix manipulations. The corrections were also the consequences of drift corrections using accelerometer, magnetometer and GPS data.

The model presented in Fig. 2 indicated that the rotation matrix was constantly checked for errors, singularities and drifts. The feedback loop was used to ensure that the nonlinearity of the matrix

https://doi.org/10.1017/S026357471400201X Published online by Cambridge University Press

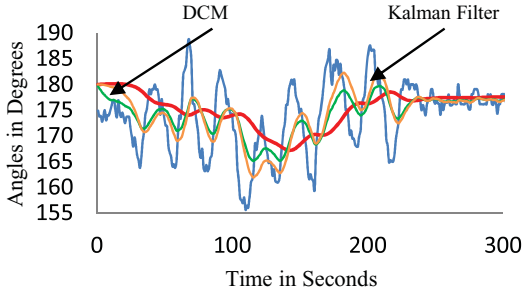

Fig. 9. Kalman filter without any unbiased gyro rate.

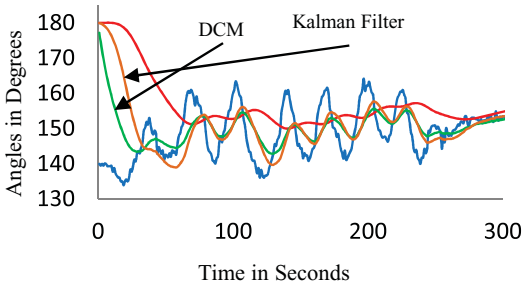

Fig. 10. Kalman filter with unbiased gyro $_{rate}$.

elements was maintained. The results were used to check whether the computational efficiency of the DCM algorithm was fast enough to be used in the autonomous marine craft navigation. The speed at which the results were accessed in real time was relative to the type of microcontroller used. Sample rate was also dependent on the type of microcontroller used. Results from Kalman filter as shown in Figs. 9 and 10 were used in validating the performance of DCM algorithm.

9. Discussion

The platform used for testing the software code and algorithm implementation was Atmega328 chip running at 20 MHz maximum speed. At ADC free running mode of 8 MHz, the sampling rate for DCM algorithm was 40 Hz. Averaging the readings made by ADC improved the sampling rate to 500 Hz. The execution time for DCM algorithm was 5 ms on Atmega328 operating at 8 MHz. The computational efficiency of quaternion and normalized rotation matrix generated results that were reliable in the development of an autonomous navigation algorithm for an unmanned marine craft. In Fig. 7, the Euler angles contained elements of drift and uncertainty. They were not reliable in the development of autonomous navigation algorithm.

The raw gyro results in Fig. 4 were used for the comparison of results in ensuring that the computational integrity of the algorithm was maintained. Rotation of IMU was predominantly in the yaw axis as indicated in Figs. 6 and 7. This was done by comparing the values from the normalized rotation matrix or quaternion with the values from raw gyro. The process was important in the evaluation of the performance of PI controller. The normalized rotation matrix or quaternion facilitated the tuning of PI controller to obtain optimum results. Equations (21–23) were scaled by PI values during the process of drift cancellation. The results shown in Figs. 9 and 10 were from the Kalman filter used for USV attitude computation. Figure 9 showed results from USV attitude computation without unbiased gyro rate, and Fig. 10 showed results from USV attitude computation with unbiased gyro rate.

10. Conclusions

The paper presented the integration of normalized rotation matrix derived from quaternion. This provided an efficient tool in the marine vehicle attitude estimation and determination devoid of

https://doi.org/10.1017/S026357471400201X Published online by Cambridge University Press

microcontroller processing capacity reduction. DCM derived from raw gyro values provided data which were unreliable as drift was present in the representation of navigation data. Quaternion and normalization of DCM eliminated singularity issues in Euler angles. The computational efficiency of quaternion and normalized DCM enabled IMU to be rotated up to and above angles which had properties of singularities in them.

The research showed that the marine vehicle navigational algorithms can be developed using data from quaternion and normalized DCM. The computational efficiency of DCM eliminated rigorous floating points associated with Kalman filter in programming microcontrollers for use in marine autonomous motion applications. The floating points in the Kalman filter computation introduced lag factors to microcontroller efficiency. The contribution made included the provision for another efficient technique in the marine vehicle attitude, heading and reference determination in real time. The use of complementary filters in the algorithm improved the accuracy of data from IMU. Integrating quaternion into DCM computations increased the computational efficiency of the USV navigational algorithm.

References

1. A. Noureldin, A. El-shafie and M. R. Taha, "Optimizing neuro-fuzzy modules for data fusion of vehicular navigation systems using temporal cross-validation," *Eng. Appl. Artif. Intell.* **20**(1), 49–61 (2007).
2. D. Loebis, R. Sutton, J. Chudley and W. Naeem, "Adaptive tuning of a Kalman filter via fuzzy logic for an intelligent AUV navigation system," *Control Eng. Pract.* **12**(12), 1531–1539 (2004).
3. G. Lee, S. Surendran and S.-H. Kim, "Algorithms to control the moving ship during harbour entry," *Appl. Math. Model.* **33**(5), 2474–2490 (2009).
4. J. Wendel, O. Meister, C. Schlaile and G. F. Trommer, "An integrated GPS/MEMS-IMU navigation system for an autonomous helicopter," *Aerosp. Sci. Technol.* **10**(6), 527–533 (2006).
5. E. M. Bitner-Gregersen and R. Skjong, "Concept for a risk based navigation decision assistant," *Mar. Struct.* **22**(2), 275–286 (2009).
6. D. E. Caron Francois, P. Denis and V. Philippe, "GPS/IMU data fusion using multisensor Kalman filtering: Introduction of contextual aspects," *Inf. Fusion* **7**(12), 221–230 (2006).
7. X. Kong, "INS algorithm using quaternion model for low cost IMU," *Robot. Auton. Syst.* **46**(1), 221–246 (2004).
8. S. de La Parra and J. Angel, "Low-cost navigation system for UAV's," *Aerosp. Sci. Technol.* **9**(6), 504–516 (2005).
9. C. Onunka and G. Bright. "A Study on Direction Cosine Matrix (DCM) for Autonomous Navigation," *Proc: 25th International Conference on CAD/CAM, Robotic & Factories of the Future, Cars & FoF 2010*, Pretoria, South Africa 1–10, 13–16 July, (2010).
10. P. C. Mark Euston, R. Mahony, J. Kim and T. Hamel, "A Complementary Filter for Attitude Estimation of a Fixed-Wing UAV," in *Proceedings of the International Conference on Intelligent Robots and Systems (IROS 2008)*, Nice,. 340–345, 22–26 Sept (2008).
11. T. H. Robert Mahony and J.-M. Pflimlin, "Nonlinear complementary filters on the special orthogonal group," *IEEE Trans. Autom. Control* **53**(5), 1203–1218, (2008).
12. R. M. Grant Baldwin, J. Trumpf, T. Hamel and T. Cheviron, "Complementary Filter Design on the Special Euclidean Group SE(3)," *Proceedings of the European Control Conference (ECC 2007)*, Kos, Greece, 1–8, 2–5 July, (2007).
13. S.-H. C. Robert Mahony and T. Hamel, "A Coupled Estimation and Control Analysis for Attitude Stabilisation of Mini Aerial Vehicles," *Proceedings of the Australasian Conference on Robotics and Automation*, Auckland, New Zeland, 1–10, 8 December, (2006).
14. J. F. Wagner and T. Wieneke, "Integrating satellite and inertial navigation–conventional and new fusion approaches," *Control Engineering Practice* **11**(5), 543–550 (2003).
15. R. Stancic and S. Graovac, "The integration of strap-down INS and GPS based on adaptive error damping," *Robot. Auton. Syst.*, **58**(10), 1117–1129 (2010).
16. J. Bijker and W. Steyn, "Kalman filter configurations for a low-cost loosely integrated inertial navigation system on an airship," *Control Eng. Pract.* **16**(12), 1509–1518 (2008).
17. W. Wang, Z.-Y. Liu and R.-R. Xie., "Quadratic extended Kalman filter approach for GPS/INS integration," *Aerosp. Sci. Technol.* **10**(8), 709–713 (2006).
18. P. B. William Premerlani, "Direction Cosine Matrix IMU: Theory," (2009). Available: http://gentlenav.googlecode.com/files/DCMDraft2.pdf, Accessed: 20 September 2009.
19. T. I. Fossen, *Guidance and Control of Ocean Vehicles* (John Wiley, West Sussex, UK, 1994).
20. G. G. Rigatos, "Sensor fusion-based dynamic positioning of ships using extended Kalman and particle filtering," Robotica **31**(3), 386–403 (2013).
21. F. Fahimi and C. Van Kleeck, "Alternative trajectory-tracking control approach for marine surface vessels with experimental verification," *Robotica* **31**(1), 25–33 (2012).

https://doi.org/10.1017/S026357471400201X Published online by Cambridge University Press

22. R. A. Soltan, H. Ashrafiuon and K. R. Muske, "ODE-based obstacle avoidance and trajectory planning for unmanned surface vessels," *Robotica* **29**(5), 691–703 (2011).
23. S. K. Sharma, W. Naeem and R. Sutton, "An autopilot based on a local control network design for an unmanned surface vehicle," *J. Navig.* **65**(2), (The Royal Institute of Navigation), 281–301 (2012).
24. A. Motwani, S. K. Sharma, R. Sutton and P. Culverhouse, "Interval Kalman filtering in navigation system design for an uninhabited surface vehicle," *J. Navig.* **66**(5), (The Royal Institute of Navigation), 639–652 (2013).
25. S. Hong, M. H. Lee, H.-H. Chun, S.-H. Kwon and J. L. Speyer, "Observability of error states in GPS/INS integration," *IEEE Trans. Veh. Technol.* **54**(2), 731–743 (2005).
26. J. Kim, J.-G. Lee, G.-I. Jee and T.-K. Sung, "Compensation of Gyroscope Errors and GPS/DR Integration," *Proceedings of the IEEE Positioning Location and Navigation Symposium*, Atlanta, GA, 464–470, 22–26, April (1996).
27. S. Han and J. Wang, "Quantization and coloured noise error modelling for inertial sensors for GPS/INS integration," *IEEE Sensors J.* **11**(6), 1493–1503 (2011).
28. E. Kralikova and R. Ravas, "Analysis of the Influence of Quantization Error at Sensor Autocalibration," *Proceedings of the 13th International Symposium on MECHATRONIKA*, Trencianske Teplice, 74–77, 2–4 June, (2010).
29. L. Stocco, S. E. Salcudean and F. Sassani, "Matrix Normalization for Optimal Robot Design," *Proceedings of the IEEE International Conference on Robotics and Automation*, Leuven, 1346–1351, 16–20 May, (1998).

https://doi.org/10.1017/S026357471400201X Published online by Cambridge University Press